Eur. Phys. J. Plus (2020) 135:851
https://doi.org/10.1140/epjp/s13360-020-00842-6

THE EUROPEAN PHYSICAL JOURNAL PLUS

Regular Article

Generalized thermoviscoelastic novel model with different fractional derivatives and multi-phase-lags

A. Soleiman[1,2,a], **Ahmed E. Abouelregal**[1,3,b], **K. M. Khalil**[1,2,c], **M. E. Nasr**[1,2,d]

[1] Department of Mathematics, College of Science and Arts, Jouf University, Gurayat, Saudi Arabia
[2] Department of Mathematics, Faculty of Science, Benha University, Benha 13518, Egypt
[3] Department of Mathematics, Faculty of Science, Mansoura University, Mansoura 35516, Egypt

Received: 12 July 2020 / Accepted: 6 October 2020

Abstract In the current investigation, we introduce a generalized modified model of thermoviscoelasticity with different fractional orders. Based on the Kelvin–Voigt model and generalized thermoelasticity theory with multi-phase-lags, the governing system equations are derived. In limited cases, the proposed model is reduced to several previous models in the presence and absence of fractional derivatives. The model is then adopted to investigate a problem of an isotropic spherical cavity, the inner surface of which is exposed to a time-dependent varying heat and constrained. The system of governing differential equations has been solved analytically by applying the technique of Laplace transform. To clarify the effects of the fractional-order and viscoelastic parameters, we depicted our numerical calculations in tables and figures. Finally, the results obtained are discussed in detail and also confirmed with those in the previous literature.

List of symbols

μ_0, λ_0	Lame's constants
μ_v, λ_v	Thermoviscoelastic relaxation times
α_t	Thermal expansion coefficient
C_e	Specific heat
$\gamma_0 = (3\lambda_0 + 2\mu_0)\alpha_t$	Thermal coupling parameter
T_0	Environmental temperature
$\theta = T - T_0$	Temperature increment
T	Absolute temperature
$\vec{u}$	Displacement vector
$e = \text{div}\,\vec{u}$	Cubical dilatation
σ_{ij}	Stress tensor

[a] e-mail: amrsoleiman@yahoo.com (corresponding author)
[b] e-mail: ahabogal@gmail.com
[c] e-mail: khalil.khalil@fsc.bu.edu.eg
[d] e-mail: mohamed.naser@fsc.bu.edu.eg

Published online: 20 October 2020

K	Thermal conductivity
ρ	Material density
Q	Heat source
t	The time
δ_{ij}	Kronecker's delta function
$\vec{E}$	Induced electric field
τ_q	Phase lag of heat flux
τ_θ	Phase lag of temperature
e_{ij}	Strain tensor
$\boldsymbol{q}$	Heat flux vector

1 Introduction

Generalized thermoelastic models have been progressed to eliminate the contradiction in the infinite velocity of heat propagation concealed in the classical dynamical coupled thermoelasticity theory [1]. In these generalized models, the basic equations contain thermal relaxation times of hyperbolic type [2–5]. Furthermore, Tzou [6–8] investigated the dual-phase-lag heat conduction theory by including two different phase delays correlating with the heat flow and temperature gradient. Chandrasekharaiah [9] introduced a generalized model improved from the heat conduction model established by Tzou [7, 8].

In the recent past, fractional calculus has been effectively applied in many fields to solve problems in electronics, wave propagation, modeling, biology, chemistry, and viscosity [10–15]. Alternative definitions and generalization of fractional derivatives were introduced by [16–18]. Furthermore, several models of thermoelasticity have been investigated with fractional derivatives by many researchers [19–24].

Recently, Abouelregal [25–27] created generalized and novel models of thermoelasticity using fractional calculus. More recently, Abouelregal et al. [28] studied generalized thermoelastic diffusion model with higher-order fractional time derivatives and four-phase-lags.

The present contribution aims to investigate a generalized two-fractional-parameter heat conduction model of thermoviscoelasticity with multi-phase-lags. According to this model and in limited cases, we can derive various classical, generalized, and fractional thermoviscoelasticity models (see Sect. 6). As an application of this model, we study an isotropic homogeneous spherical cavity whose inner surface is subjected to a time-dependent varying heat and constrained. Moreover, the analytical solution for various physical fields, using the Laplace transform procedure, is obtained. To clarify the effects of the fractional-order and viscoelastic parameters, we depicted our numerical calculations in tables and figures. Finally, the results obtained are discussed in detail and also confirmed with those in the previous literature.

2 Fractional thermoviscoelastic model with multi-phase-lags

Here, we investigate an advanced thermoviscoelastic model which generalizes the Kelvin–Voigt model. In this case, the basic equations of motion, constitutive equations, strain, and displacement relations based on the theory of thermoviscoelastic for a homogeneous and isotropic thermoviscoelastic solid are [29, 30]

$$\begin{gathered}\sigma_{ij}=2\mu_m e_{ij}+\delta_{ij}\left[\lambda_m e_{kk}-\gamma_m\theta\right]\\ 2e_{ij}=u_{j,i}+u_{i,j}\\ \mu_m u_{i,jj}+(\lambda_m+\mu_m)u_{j,ij}-\gamma_m\theta_{,i}+F_i=\rho\ddot{u}_i\end{gathered}\tag{1}$$

The parameters μ_m and λ_m are assumed to be in the following generalized forms:

$$\begin{gathered}\mu_m=\mu_0\left(1+\mu_v^\delta\frac{\partial^\delta}{\partial t^\delta}\right)\\ \lambda_m=\lambda_0\left(1+\lambda_v^\delta\frac{\partial^\delta}{\partial t^\delta}\right)\end{gathered}\tag{2}$$

where $0<\delta\le 1$. Note that when $\delta=1$, the classical Kelvin–Voigt model is obtained. Hence, the coupling modulus γ_m has the form

$$\gamma_m=\gamma_0\left(1+\gamma_v^\delta\frac{\partial^\delta}{\partial t^\delta}\right)\tag{3}$$

where $\gamma_0=(3\lambda_0+2\mu_0)\alpha_t$ and $\gamma_v=\frac{(3\lambda_0\lambda_v^\delta+2\mu_0\mu_v^\delta)\alpha_t}{\gamma_0}$.

On the other hand, the usual theory of heat conduction based on Fourier's law for infinite heat propagation speed is given by [1]

$$\vec{q}(x,t)=-K\nabla\theta(x,t)\tag{4}$$

Recently, a generalized dual-phase-lag model has been introduced by Tzou [8]:

$$\left(1+\tau_q\frac{\partial}{\partial t}+\frac{\tau_q^2}{2!}\frac{\partial^2}{\partial t^2}\right)\vec{q}=-K\left(1+\tau_\theta\frac{\partial}{\partial t}\right)\nabla\theta\tag{5}$$

Because there is a deficiency in the traditional Kelvin–Voigt model in describing some physical phenomena of viscous materials in a manner that differs greatly from laboratory experiments, several modifications have been proposed. Fractional-order models illustrate the viscoelastic material behavior through corresponding fractional differential equations that are physically appropriate.

In this work, we will introduce a new thermoelastic model of fractional heat conduction law, where the generalized Fourier's law is modified by using the concepts of fractional Taylor's series expansion proposed by Jumarie [23]. In this case, the time fractional dual-phase-lag model is obtained as

$$\left(1+\frac{\tau_q^\alpha}{\alpha!}\frac{\partial^\alpha}{\partial t^\alpha}+\frac{\tau_q^{2\alpha}}{2\alpha!}\frac{\partial^{2\alpha}}{\partial t^{2\alpha}}\right)\vec{q}=-K\left(1+\frac{\tau_\theta^\alpha}{\alpha!}\frac{\partial^\alpha}{\partial t^\alpha}\right)\nabla\theta\tag{6}$$

where $\tau_q\ge\tau_\theta>0$ and $0<\alpha\le 1$.

We applied the Riemann–Liouville fractional integral to the previous equation which is defined as a generalization of the convolution-type integral [13, 15]:

$$I^\alpha f(t)=\int_0^t\frac{(t-\xi)^{\alpha-1}}{\Gamma(\alpha)}f(\xi)d\xi\tag{7}$$

where I^α is the Riemann–Liouville integral operator of order α, $\Gamma(\alpha)$ is the Gamma function, $f(t)$ is a Lebesgue integrable function and t is the time. Hence, for absolutely continuous function $f(t)$, we have

$$\lim_{\alpha\to 1}\left(\frac{\mathrm{d}^\alpha}{\mathrm{d}t^\alpha}f(t)\right)=f'(t)\tag{8}$$

The energy balance equation with heat source is given by [28, 29]

$$\rho C_e \frac{\partial \theta}{\partial t} + \gamma_m T_0 \frac{\partial}{\partial t}(\mathrm{div}\vec{u}) - \rho \mathrm{Q} = -\mathrm{div}\overrightarrow{q} \tag{9}$$

where C_e denotes the specific heat at constant strain, γ_m is defined by Eq. (3) and Q is the heat supply. Therefore, from Eqs. (6) and (9), we get

$$\left(1 + \frac{\tau_q^\alpha}{\alpha!}\frac{\partial^\alpha}{\partial t^\alpha} + \frac{\tau_q^{2\alpha}}{2\alpha!}\frac{\partial^{2\alpha}}{\partial t^{2\alpha}}\right)\left[\rho C_e \frac{\partial \theta}{\partial t} + \gamma_m T_0 \frac{\partial}{\partial t}(\mathrm{div}\vec{u}) - \rho Q\right] = K\left(1 + \frac{\tau_\theta^\alpha}{\alpha!}\frac{\partial^\alpha}{\partial t^\alpha}\right)\nabla^2\theta \tag{10}$$

This equation defines an advanced thermoviscoelastic fractional model with a dual-phase-lag of fractional parameter α, and we denoted by **FMVDPL**. This model has widely used in chemistry, biology, modeling and identification, electronics, wave propagation, and viscoelasticity [10–15].

3 An application to the constructed model

We are interested in studying an isotropic homogeneous spherical cavity of radius a whose inner surface is exposed to a time-dependent varying heat and constrained. We also suppose that there are no sources or body forces applied to the body. We will use the spherical system of coordinates (r, ϑ, φ) as depicted in the following figure.

According to symmetry, all the studied functions are to be considered depending on the distance r and the time t. The displacement vector has the components

$$u_r = u(r, t), u_\vartheta(r, t) = u_\varphi(r, t) = 0 \tag{11}$$

The dilatation e has the form

$$e = \frac{1}{r^2}\frac{\partial\left(r^2 u\right)}{\partial r} \tag{12}$$

The constitutive equation is given by

$$\sigma_{rr} = 2\mu_m \frac{\partial u}{\partial r} + \lambda_m e - \gamma_m \theta \tag{13}$$

$$\sigma_{\vartheta\vartheta} = \sigma_{\varphi\varphi} = 2\mu_m \frac{u}{r} + \lambda_m e - \gamma_m \theta \tag{14}$$

Also, the equation of motion without external force F_i has the form

$$\frac{\partial \sigma_{rr}}{\partial r} + \frac{2}{r}(\sigma_{rr} - \sigma_{\vartheta\vartheta}) = \rho \frac{\partial^2 u}{\partial t^2} \tag{15}$$

From which together with Eqs. (13) and (14), the equation of motion has the form

$$(\lambda_m + 2\mu_m)\frac{\partial e}{\partial r} - \gamma_m \frac{\partial \theta}{\partial r} = \rho \frac{\partial^2 \mathrm{u}}{\partial t^2} \tag{16}$$

Applying the operator $\frac{1}{r^2}\frac{\partial}{\partial r}\left(r^2\right)$ to both sides of the above equation taking into account Eq (12) and the expression of the Laplace's operator $\nabla^2 = \frac{\partial^2}{\partial r^2} + \frac{2}{r}\frac{\partial}{\partial r} = \frac{1}{r^2}\frac{\partial}{\partial r}\left(r^2 \frac{\partial}{\partial r}\right)$ in the spherical polar coordinates, we obtain

$$(\lambda_m + 2\mu_m)\nabla^2 e - \gamma_m \nabla^2 \theta = \rho \frac{\partial^2 e}{\partial t^2} \tag{17}$$

In view of Eq. (10), the modified equation of heat conduction with fractional derivatives and phase lags with $Q = 0$ can be written as

$$\left(1 + \frac{\tau_q^\alpha}{\alpha!}\frac{\partial^\alpha}{\partial t^\alpha} + \frac{\tau_q^{2\alpha}}{2\alpha!}\frac{\partial^{2\alpha}}{\partial t^{2\alpha}}\right)\left[\rho C_e\frac{\partial \theta}{\partial t} + \gamma_m T_0\frac{\partial e}{\partial t}\right] = K\left(1 + \frac{\tau_\theta^\alpha}{\alpha!}\frac{\partial^\alpha}{\partial t^\alpha}\right)\nabla^2\theta \tag{18}$$

We introduce the following non-dimensional variables

$$\begin{gathered}\left\{r', u\prime\right\} = c_0\eta\{x, u\}, \left\{t\prime, \mu_v\prime, \lambda_v\prime, \tau_q\prime, \tau_\theta\prime\right\} = c_0^2\eta\left\{t, \mu_v, \lambda_v, \tau_q, \tau_\theta\right\};\\ \theta\prime = \frac{\gamma_0\theta}{\lambda_0+2\mu_0}, \sigma\prime_{ij} = \frac{\sigma_{ij}}{\mu_0}, c_0 = \sqrt{\frac{\lambda_0+2\mu_0}{\rho}}, \eta = \frac{\rho C_e}{K}.\end{gathered} \tag{19}$$

Under the above non-dimensional forms together with dropping the primes for convenience, Eqs. (17), (18), and (13) become

$$\left(1 + \beta_v\frac{\partial^\delta}{\partial t^\delta}\right)\nabla^2 e - \left(1 + \gamma_v^\delta\frac{\partial^\delta}{\partial t^\delta}\right)\nabla^2\theta = \frac{\partial^2 e}{\partial t^2} \tag{20}$$

$$\left(1 + \frac{\tau_q^\alpha}{\alpha!}\frac{\partial^\alpha}{\partial t^\alpha} + \frac{\tau_q^{2\alpha}}{2\alpha!}\frac{\partial^{2\alpha}}{\partial t^{2\alpha}}\right)\left[\frac{\partial \theta}{\partial t} + \varepsilon\left(1 + \gamma_v^\delta\frac{\partial^\delta}{\partial t^\delta}\right)\frac{\partial e}{\partial t}\right] = \left(1 + \frac{\tau_\theta^\alpha}{\alpha!}\frac{\partial^\alpha}{\partial t^\alpha}\right)\nabla^2\theta \tag{21}$$

$$\begin{aligned}\sigma_{rr} &= 2\left(1 + \mu_v^\delta\frac{\partial^\delta}{\partial t^\delta}\right)\frac{\partial u}{\partial r} + \left(\beta^2 - 2\right)\left(1 + \lambda_v^\delta\frac{\partial^\delta}{\partial t^\delta}\right)e - \beta^2\left(1 + \gamma_v^\delta\frac{\partial^\delta}{\partial t^\delta}\right)\theta\\ \sigma_{\vartheta\vartheta} &= 2\left(1 + \mu_v^\delta\frac{\partial^\delta}{\partial t^\delta}\right)\frac{u}{r} + \left(\beta^2 - 2\right)\left(1 + \lambda_v^\delta\frac{\partial^\delta}{\partial t^\delta}\right)e - \beta^2\left(1 + \gamma_v^\delta\frac{\partial^\delta}{\partial t^\delta}\right)\theta\end{aligned} \tag{22}$$

where

$$\beta_v = \frac{\lambda_0\lambda_v^\delta + 2\mu_0\mu_v^\delta}{\lambda_0 + 2\mu_0}, \beta^2 = \frac{\lambda_0 + 2\mu_0}{\mu_0}, \varepsilon = \frac{\gamma_0^2 T_0}{\rho C_e(\lambda_0 + 2\mu_0)}. \tag{23}$$

We have dropped the primes in Eqs. (20)–(23) for convenience and clarity of the problem.

4 The initial and boundary conditions

We suppose that the medium initially is at rest so that initial conditions of the problem have the form:

$$\begin{aligned}e(r, t)|_{t=0} &= \left.\frac{\partial e(r,t)}{\partial t}\right|_{t=0} = 0\\ \theta(r, t)|_{t=0} &= \left.\frac{\partial \theta(r,t)}{\partial t}\right|_{t=0} = 0\end{aligned} \tag{24}$$

We suppose that the boundary of the cavity $r = a$ is constraint and is subjected to a constant heat flux. So, the following boundary conditions hold

$$u(r, t) = 0,\ \ q(r, t) = q_0 H(t) \text{ at } r = a, \tag{25}$$

where q_0 is the dimensionless constant heat flux and $H(t)$ is the Heaviside's unit step function. Due to Eq. (19), the boundary conditions have the form:

$$\begin{gathered}u(a, t) = 0,\\ q_0\left(1 + \frac{\tau_q^\alpha}{\alpha!}\frac{\partial^\alpha}{\partial t^\alpha} + \frac{\tau_q^{2\alpha}}{2\alpha!}\frac{\partial^{2\alpha}}{\partial t^{2\alpha}}\right)H(t) = -\left(1 + \frac{\tau_\theta^\alpha}{\alpha!}\frac{\partial^\alpha}{\partial t^\alpha}\right)\frac{\partial \theta(r, t)}{\partial r}, \text{ at } r = a.\end{gathered} \tag{26}$$

5 Transform solution

Applying the Laplace transform for Eqs. (20)–(23), taking into account the considered initial conditions (24), we obtain:

$$\nabla^2\bar{e} - q_1\nabla^2\bar{\theta} = q_2\bar{e} \tag{27}$$

$$q_3\bar{\theta} + q_4\bar{e} = q_5\nabla^2\bar{\theta}. \tag{28}$$

$$\begin{aligned}\sigma_{rr} &= 2q_6\tfrac{\mathrm{d}\bar{u}}{\mathrm{d}r} + \left(\beta^2 - 2\right)q_7\bar{e} - \beta^2 q_8\bar{\theta}\\ \sigma_{\vartheta\vartheta} &= 2q_6\tfrac{\bar{u}}{r} + \left(\beta^2 - 2\right)q_7\bar{e} - \beta^2 q_8\bar{\theta},\end{aligned} \tag{29}$$

where

$$q_1 = \frac{\left(1+\gamma_v^\delta s^\delta\right)}{\left(1+\beta_v s^\delta\right)},\ q_2 = \frac{s^2}{\left(1+\beta_v s^\delta\right)},\ q_3 = s\left(1+\frac{\tau_q^\alpha}{\alpha!}s^\alpha + \frac{\tau_q^{2\alpha}}{2\alpha!}s^{2\alpha}\right)$$
$$q_4 = \varepsilon\left(1+\gamma_v^\delta s^\delta\right)q_3,\ q_5 = \left(1+\frac{\tau_\theta^\alpha}{\alpha!}s^\alpha\right),\ q_6 = \left(1+\mu_v^\delta s^\delta\right),$$
$$q_7 = \left(1+\lambda_v^\delta s^\delta\right),\ q_8 = \left(1+\gamma_v^\delta s^\delta\right) \tag{30}$$

In view of Eqs. (27) and (28), we get

$$\left(\nabla^4 - A\nabla^2 + B\right)\left\{\bar{\theta}, \bar{e}\right\} = 0, \tag{31}$$

where

$$A = \frac{q_3 + q_1q_4 + q_2q_5}{q_5},\ B = \frac{q_2q_3}{q_5}. \tag{32}$$

Introducing m_i, $(i = 1, 2)$ into Eq. (31), one get

$$\left(\nabla^2 - m_1^2\right)\left(\nabla^2 - m_2^2\right)\left\{\bar{\theta}, \bar{e}\right\} = 0, \tag{33}$$

where m_1^2 and m_2^2 are the roots of the characteristic equation

$$m^4 + Am^2 - B = 0. \tag{34}$$

Using the substitution $f = \frac{\bar{e}}{\sqrt{r}}$ and using the fact that the modified Bessel function $K_{1/2}(z) = \frac{e^{-z}\sqrt{\frac{\pi}{2}}}{\sqrt{z}}$, the solutions of Eq. (33) taking into account the regularity conditions that $\bar{\theta}, \bar{e} \to 0$ as $r \to \infty$ have the form

$$\left\{\bar{e}, \bar{\theta}\right\} = \sum_{i=1}^{2}\{1, L_i\}A_i(s)\frac{e^{-m_i r}}{r}\sqrt{\frac{\pi}{2m_i}} \tag{35}$$

where A_i $(i = 1, 2)$ are some parameters depending on the parameter s and L_i is given by

$$L_i = \frac{m_i^2 - q_2}{q_1 m_i^2}. \tag{36}$$

Using Eqs. (12) and (35), we get

$$\bar{u} = -\sum_{i=1}^{2}\frac{1}{m_i}\left(1+\frac{1}{m_i r}\right)A_i(s)\frac{e^{-m_i r}}{r}\sqrt{\frac{\pi}{2m_i}} \tag{37}$$

Now, from Eqs. (35), (36), and (29), we have

$$\begin{aligned}\sigma_{rr} &= \sum_{i=1}^{2}\left[2q_6\left(1+\tfrac{2}{m_i r}+\tfrac{2}{m_i^2 r^2}\right)+\left(\beta^2-2\right)q_7-\beta^2 q_8 L_i\right]A_i(s)\tfrac{e^{-m_i r}}{r}\sqrt{\tfrac{\pi}{2m_i}} \\ \sigma_{\vartheta\vartheta} &= \sum_{i=1}^{2}\left[-2q_6\left(\tfrac{1}{m_i r}+\tfrac{1}{m_i^2 r^2}\right)+\left(\beta^2-2\right)q_7-\beta^2 q_8 L_i\right]A_i(s)\tfrac{e^{-m_i r}}{r}\sqrt{\tfrac{\pi}{2m_i}}.\end{aligned} \tag{38}$$

Under Laplace transform, the boundary condition (26) becomes

$$\begin{aligned}&\bar{u}(r,s)=0,\\ &\frac{\mathrm{d}\bar{\theta}(r,s)}{\mathrm{d}r}=-\frac{q_0 q_3}{s^2 q_5}=-G(s),\ \text{ at } r=a.\end{aligned} \tag{39}$$

Consequently, we get

$$\begin{aligned}\sum_{i=1}^{2}\left(\frac{1}{m_i a}+\frac{1}{m_i^2 a^2}\right)A_i(s)e^{-m_i a}\sqrt{\frac{\pi}{2m_i}}&=0\\ \sum_{i=1}^{2}L_i A_i(s)\left(\frac{1}{a^2}+\frac{m_i}{a}\right)e^{-m_i a}\sqrt{\frac{\pi}{2m_i}}&=\frac{q_0 q_3}{s^2 q_5}\end{aligned} \tag{40}$$

Therefore, from the above system, we can determine the parameters A_1, A_2 in the Laplace transform domain and hence the physical fields of the medium.

Finally, to have the solutions of the studied fields in the physical domain, we use a proper and effective numerical method depending on a Fourier series expansion [31]. In this method, any function in the Laplace domain can be reversed to the time domain as

$$\mathcal{M}(r,t)=\frac{e^{ct}}{t}\left(\frac{1}{2}\bar{\mathcal{M}}(r,c)+\mathrm{Re}\sum_{n=1}^{m}\bar{\mathcal{M}}\left(r,c+\frac{in\pi}{t}\right)(-1)^n\right), \tag{41}$$

where m is a finite number of terms, Re is the real part and i is imaginary number unit. For faster convergence, numerous numerical experiments have shown that the value of c fulfills the relation $ct \cong 4.7$ [31].

6 Special cases of modified fractional thermoviscoelastic model

In Sect. 2, we investigated a generalized modified model of thermoviscoelasticity with different fractional orders. In limited cases, the proposed model is reduced to several previous models in the presence and absence of fractional.

The obtained models are listed in the following table:

	Name of model	Abbreviated name	Conditions
1	Classical thermoelastic model	CTE	$\tau_q = \tau_\theta = 0,$ $\mu_v = \lambda_v = 0$
2	Lord–Shulman model	LS	$\tau_q > 0,\ \alpha \to 0,\ \tau_\theta = 0,$ $\mu_v = \lambda_v = 0$
3	Dual-phase-lag model	DPL	$\tau_q \geq \tau_\theta > 0,\ \alpha \to 1,$ $\mu_v = \lambda_v = 0$
4	Classical thermoviscoelastic model	VCTE	$\tau_q = \tau_\theta = 0,$ $\mu_v \neq 0 \neq \lambda_v,\ \delta \to 1$
5	Viscoelastic Lord–Shulman model	VLS	$\tau_q > 0,\ \alpha \to 0,\ \tau_\theta = 0,$ $\mu_v \neq 0 \neq \lambda_v,\ \delta \to 1$
6	Viscoelastic dual-phase-lag model	VDPL	$\tau_q \geq \tau_\theta > 0,\ \alpha \to 1,$ $\mu_v \neq 0 \neq \lambda_v,\ \delta \to 1$
7	Classical fractional thermoviscoelastic model	MVCTE	$\tau_q = \tau_\theta = 0,$ $\mu_v \neq 0 \neq \lambda_v,\ 0 < \delta < 1$
8	Fractional thermoviscoelastic Lord–Shulman model	MVLS	$\tau_q > 0,\ \alpha \to 0,\ \tau_\theta = 0,$ $\mu_v \neq 0 \neq \lambda_v,\ 0 < \delta < 1$
9	Fractional thermoviscoelastic dual-phase-lag model	MVDPL	$\tau_q \geq \tau_\theta > 0,\ \alpha \to 1,$ $\mu_v \neq 0 \neq \lambda_v,\ 0 < \delta < 1'$
10	Fractional thermoviscoelastic Lord–Shulman model with one fractional order	FMVLS	$\tau_q > 0,\ 0 < \alpha < 1,\ \tau_\theta = 0,$ $\mu_v \neq 0 \neq \lambda_v,\ 0 < \delta < 1$
11	Fractional thermoviscoelastic dual-phase-lag with two fractional orders	FMVDPL	$\tau_q \geq \tau_\theta > 0,\ 0 < \alpha < 1,$ $\mu_v \neq 0 \neq \lambda_v,\ 0 < \delta < 1$

7 Numerical results and verification

The aim of this section is to describe and confirm results achieved in the previous sections. Also, we present the numerical results. For the numerical calculations, we use the value of the copper material at $T_0 = 293\text{K}$ as [32]

$$\lambda_0 = 7.76 \times 10^{10}\ \text{kg m}^{-1}\text{s}^{-2},\ \mu_0 = 3.86 \times 10^{10}\ \text{kg m}^{-1}\text{s}^{-2},\ \varepsilon = 0.0168$$
$$\rho = 8954\ \text{kg m}^{-3},\ K = 386\ \text{W m}^{-1}\text{K}^{-1},\ C_e = 3.381\ \text{J kg K}^{-1}.$$

The obtained results are accessible in Tables 1, 2, 3, and 4 and graphically in Figs. 2, 3, 4, 5, 6, 7, 8, 9, 10, 11, 12, and 13 at different values of the radius $r(1 \leq r \leq 2)$ and different values of the fractional parameter α at $t = 0.12$, when the dual-phase-lags $\tau_\theta = 0.05$ and $\tau_q = 0.07$, together with different values of the fractional $\delta(0 < \delta \leq 1)$, when the thermoviscoelastic relaxation times $\mu_v = 0.2$ and $\lambda_v = 0.3$. The Mathematica programming language is used within our numerical calculations. Comparisons are accomplished with the expected results predicted by all the models mentioned. Furthermore, the numerical calculations are prepared for three directions.

Table 1 The temperature θ in different models

R	MVCTE	MVLS	FMVLS	DPL	VDPL	MVDPL	FMVDPL
1	0.44921	0.717551	0.523342	0.51395	1.45383	0.97353	0.735779
1.1	0.0904456	0.0884112	0.0903404	0.0926206	0.270999	0.180296	0.178391
1.2	0.0275086	0.022652	0.0272336	0.0262543	0.0787153	0.052539	0.0631869
1.3	0.00878854	0.00629856	0.00863144	0.00794257	0.0240794	0.0161888	0.0228682
1.4	0.0030161	0.00200747	0.0029468	0.00229933	0.00800624	0.0054292	0.00861401
1.5	0.00115344	0.000778807	0.00112568	0.000792886	0.00302099	0.00206887	0.0034414
1.6	0.000515286	0.000379713	0.000504548	0.000347676	0.00134694	0.000939926	0.00150739
1.7	0.000273986	0.000223933	0.000269809	0.00010552	0.000713666	0.000513277	0.000746289
1.8	0.000166774	0.00014697	0.000165077	0.000061171	0.000431384	0.000319642	0.000417548
1.9	0.000109249	0.00010044	0.000108502	1.95955E − 05	0.000281204	0.000212404	0.000255806
2	7.37661E − 05	6.92564E − 05	7.34002E − 05	1.45436E − 05	0.000189712	0.000144521	0.000165392

Table 2 The displacement u in different models

R	MVCTE	MVLS	FMVLS	DPL	VDPL	MVDPL	FMVDPL
1	0	0	0	0	0	0	0
1.1	0.0117357	0.0126337	0.0117921	0.00855796	0.0114391	0.0119813	0.0108112
1.2	0.00780022	0.00794909	0.00781164	0.00546585	0.00749248	0.00784739	0.00757933
1.3	0.00449065	0.00446018	0.00448936	0.0024797	0.00424934	0.00448419	0.00449936
1.4	0.00253308	0.00249078	0.00253043	0.000980934	0.00236675	0.00252142	0.00257632
1.5	0.00142297	0.00139417	0.00142106	0.00049085	0.00131892	0.00141466	0.00145712
1.6	0.000799972	0.000782697	0.000798804	0.000199562	0.000737487	0.000794905	0.000821714
1.7	0.00045206	0.000442015	0.000451377	9.00424E − 05	0.000414489	0.000449094	0.000465043
1.8	0.000257248	0.000251437	0.000256851	0.00004112	0.000234389	0.000255528	0.000264847
1.9	0.000147331	0.000143963	0.000147101	1.62384E − 05	0.000133344	0.000146333	0.000151759
2	8.48152E − 05	8.28554E − 05	8.46809E − 05	8.18166*10^-6	7.62577E − 05	0.000084234	8.73975E − 05

Table 3 The stress σ_{rr} in different models

R	MVCTE	MVLS	FMVLS	DPL	VDPL	MVDPL	FMVDPL
1	− 0.960435	− 1.89655	− 1.35546	− 0.305043	− 0.249751	− 1.05607	− 0.781745
1.1	− 0.432984	− 0.437634	− 0.433153	− 0.152108	− 0.402529	− 0.434445	− 0.426114
1.2	− 0.193391	− 0.19112	− 0.193278	− 0.0437565	− 0.187782	− 0.192786	− 0.195516
1.3	− 0.077998	− 0.0763971	− 0.0779012	− 0.0360416	− 0.0766554	− 0.0775365	− 0.0799091
1.4	− 0.0357111	− 0.0349077	− 0.0356565	− 0.0093899	− 0.0338459	− 0.0354748	− 0.0367345
1.5	− 0.0169451	− 0.0165624	− 0.0169186	− 0.00261567	− 0.0157785	− 0.0168319	− 0.0174441
1.6	− 0.00795976	− 0.00777733	− 0.00794723	− 0.000737426	− 0.00739899	− 0.00790568	− 0.00819968
1.7	− 0.00376065	− 0.00367281	− 0.00375465	− 0.000202832	− 0.00347771	− 0.0037346	− 0.00387654
1.8	− 0.00180024	− 0.00175757	− 0.00179732	− 5.51197E − 05	− 0.0016487	− 0.00178758	− 0.00185662
1.9	− 0.000869582	− 0.0008487	− 0.000868149	− 4.73336E − 05	− 0.000788737	− 0.000863385	− 0.000897188
2	− 0.000422467	− 0.000412188	− 0.000421761	− 1.38326E − 05	− 0.000379934	− 0.000419416	− 0.000436067

Table 4 The stress $\sigma_{\varphi\varphi}$ in different models

R	MVCTE	MVLS	FMVLS	DPL	VDPL	MVDPL	FMVDPL
1	− 0.798344	− 1.77644	− 1.20717	− 0.118082	− 3.02727	− 0.897619	− 0.617713
1.1	− 0.106629	− 0.102916	− 0.0983838	− 0.05381	− 0.282499	− 0.102138	− 0.0996806
1.2	− 0.0579508	− 0.0565845	− 0.0576664	− 0.0393677	− 0.15885	− 0.0575819	− 0.0562724
1.3	− 0.0363023	− 0.0334645	− 0.0361369	− 0.0139612	− 0.0978684	− 0.0356266	− 0.0381419
1.4	− 0.0241061	− 0.0214533	− 0.0239467	− 0.0101437	− 0.0640142	− 0.0234289	− 0.0263327
1.5	− 0.0167594	− 0.0147457	− 0.0166334	− 0.00807413	− 0.0442144	− 0.0162201	− 0.01868
1.6	− 0.0120392	− 0.0106409	− 0.0119488	− 0.0069888	− 0.0318746	− 0.0116498	− 0.01352
1.7	− 0.00883401	− 0.00790502	− 0.00877234	− 0.00644157	− 0.0236805	− 0.00856629	− 0.00991287
1.8	− 0.00657679	− 0.0059722	− 0.00653584	− 0.0017874	− 0.017953	− 0.00639725	− 0.00733948
1.9	− 0.00495975	− 0.00456822	− 0.00493282	− 0.0016536	− 0.0138098	− 0.00484047	− 0.005491
2	− 0.00379586	− 0.00354047	− 0.00377807	− 0.00161209	− 0.010753	− 0.00371645	− 0.00416426

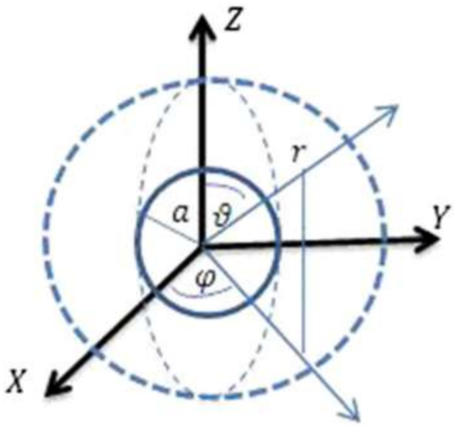

Fig. 1 Schematic diagram for spherical cavity

7.1 Comparison between different models of thermoviscoelasticity

This section is devoted to studying the distributions of the physical fields for the generalized theory with dual-phase-lags (DPL) and the modified fractional thermoviscoelastic models (MVCTE, MVLS, and MVDPL) with parameter δ, together with the generalized fractional thermoviscoelastic models (FMVLS and FMVDPL) with parameters δ, α. The obtained results are represented in Tables 1, 2, 3, and 4 and Figs. 1, 2, 3, and 4 for the field quantities corresponding to different values of the radius $r(1 \leq r \leq 2)$ at $t = 0.12$, when the dual-phase-lags $\tau_\theta = 0.05$, $\tau_q = 0.07$ with the fractional parameter $\alpha = 0.8$, and $\mu_v = 0.2$, $\lambda_v = 0.3$ with $\delta = 0.9$. These tables emphasize that the physical quantities depend not only on the time t and the radius r, but also on the fractional parameters δ, α.

Table 1 presents the variation of temperature θ, for different models of thermoelasticity. Through the table above, we note that the variations of temperature are observed to be sensitive to the parameter α. The fractional models of thermoviscoelasticity (MVCTE, MVLS, FMVLS, MDPL, MVDPL, FMVDPL) give significantly different results than the DPL model. Furthermore, the above results related to the DPL model and its modified fractional models are plotted in the following figure.

Figure 2 depicts that the variation of temperature θ in all the models (DPL, VDPL, MVDPL, FMVDPL) decreases with increasing the radius r for $1 < r < 2$. Also, we conclude that the maximum point of the temperature curve for the models (VDPL, MVDPL, FMVDPL) is bigger than that for model (DPL). It is manifested from the figure that the values of the temperature converge to zero when the radius r tends to 2, which agrees with the boundary conditions.

The variation of the displacement u in the context of seven models of thermoelasticity is obtained in Table 2. It was found that the values of the parameter α play a significant role in changing the displacement value. As visible from Table 2, the displacement reaches minimum value ($u = 0$) on the boundary at $r = 1$, which agrees with the boundary conditions. Finally, the above results related to DPL model and its modified fractional models are schemed in the following figure.

From Fig. 3, we observe that the variation of displacement u in all the models (DPL, VDPL, MVDPL, and FMVDPL) decreases with increasing the radius r for $1 < r$. Also, in view of Fig. 3 we conclude that the amplitude of the displacement u for all the models is

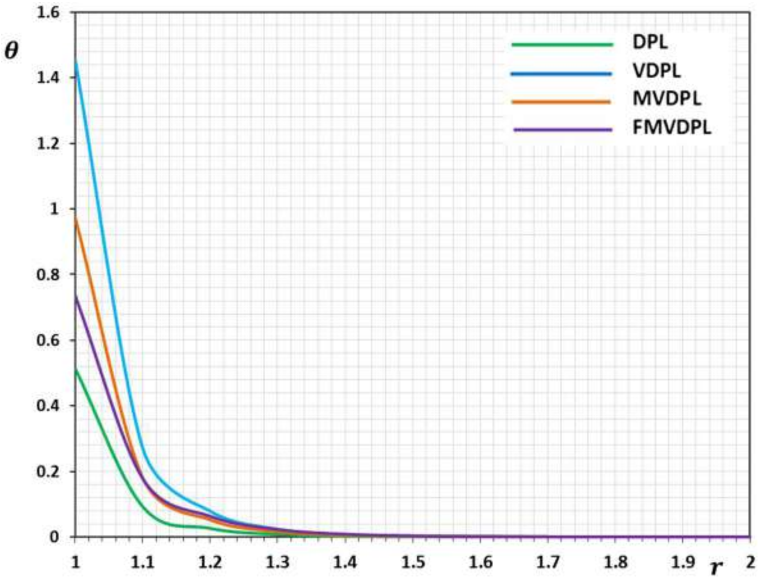

Fig. 2 The variation of temperature θ in different models related to DPL model

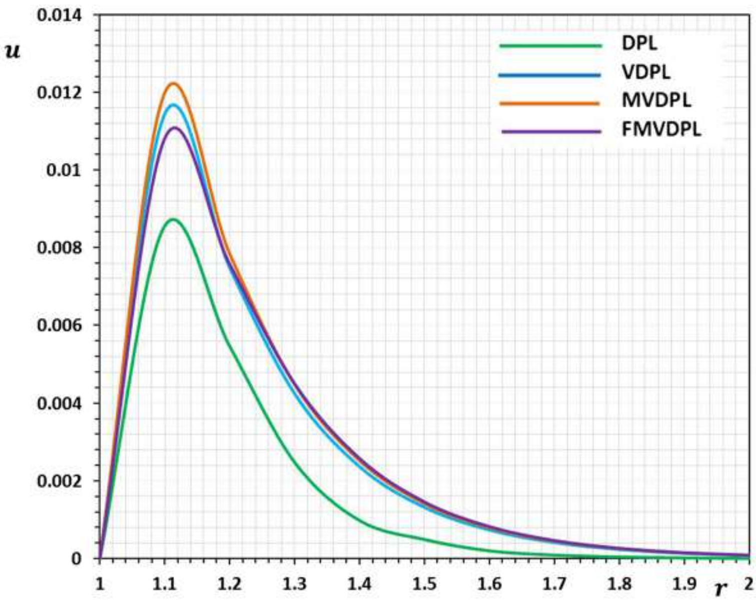

Fig. 3 The variation of displacement u in different models related to DPL model

bigger than that for the DPL model. Moreover, we find that the values of the displacement converge to zero when r tends to 2 which agree with the boundary condition.

Table 3 and Fig. 4 display the variations of stress σ_{rr} against the radius for different values of the fractional parameter α. Also, Fig. 4 emphasizes that the depth of the stress for the

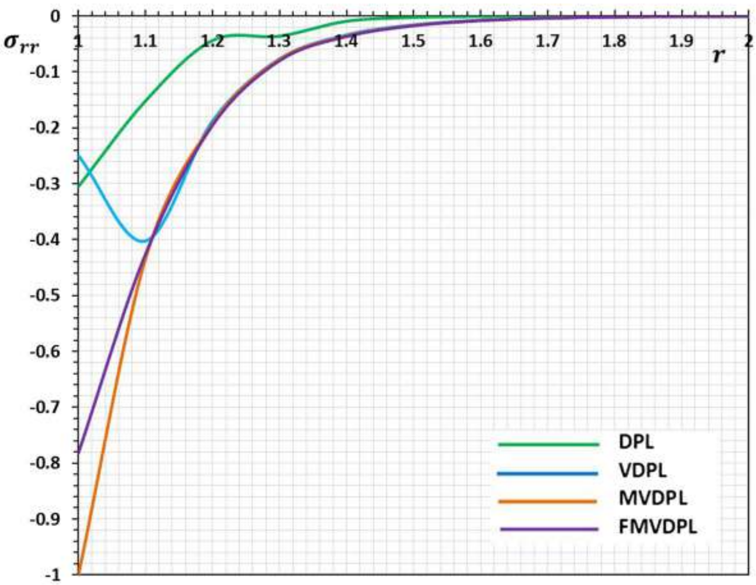

Fig. 4 The variation of the stress σ_{rr} in different models related to DPL model

models (VDPL, MVDPL, FMVDPL) is bigger than that for dual-phase-lags (DPL) model. Furthermore, we observe that the values of the stress σ_{rr} converge to zero when r tends to 2.

Similarly, Table 4 and Fig. 5 describe the variations of stress $\sigma_{\varphi\varphi}$ against the radius with different values of the fractional parameter α. Also, Fig. 5 shows that the depth of the stress for the models [VDPL, MVDPL, FMVDPL] is bigger than that for dual-phase-lags (DPL) model. Also, we see that the values of the stress $\sigma_{\varphi\varphi}$ converge to zero when r tends to 2.

7.2 The effect of the fractional parameters δ, α on the physical fields

This section is devoted to discuss how the fractional parameters δ, α act on the field variables. The obtained results are represented in Figs. 6, 7, 8, and 9 for the field quantities corresponding to different values of the radius $r(1 \leq r \leq 2)$ at $t = 0.12$, and different values for the fractional parameters δ, α, when the dual-phase-lags $\tau_\theta = 0.05$, $\tau_q = 0.07$, together with $\mu_v = 0.2$, $\lambda_v = 0.3$. These figures emphasize that the physical quantities depend not only on the radius r, but also on the fractional parameters δ, α.

It is evident from Figs. 6, 7, 8, and 9 that the different values to the fractional parameters δ, α have clearly effect on the temperature, displacement, and the stress. Also, we observe that the values of the physical quantities converge to zero when r tends to 2, which is in quite good agreement with the regularity boundary conditions.

7.3 The effect of the time on the physical fields

This section is devoted to showing the effect of the time t on all the field variables. In this case, we take the dual-phase-lags $\tau_\theta = 0.05$, $\tau_q = 0.07$ when the fractional parameter $\alpha = 0.7$ and $\mu_v = 0.2$, $\lambda_v = 0.3$ with $\delta = 0.7$. For a comparison of the results, the temperature, the

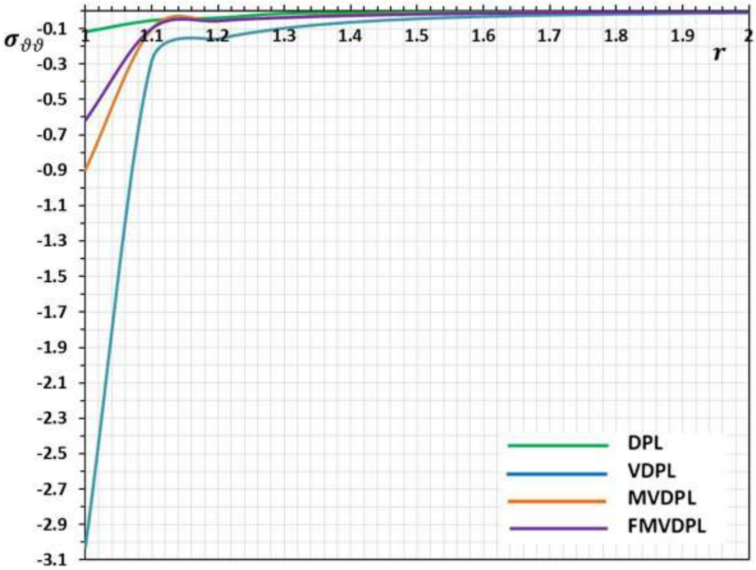

Fig. 5 The variation of the stress $\sigma_{\varphi\varphi}$ in different models related to DPL model

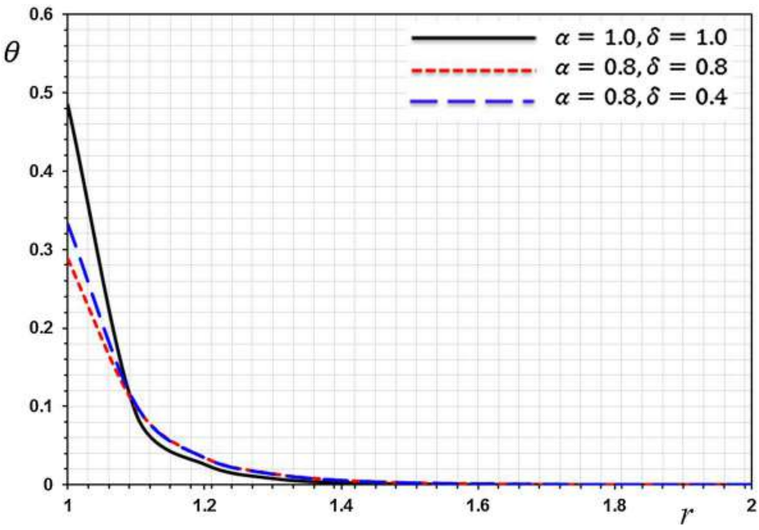

Fig. 6 The variation of temperature θ with different values of the fractional parameters δ, α

displacement, and thermal stresses are presented in Figs. 10, 11, 12, and 13. It is seen from the figures that these distributions are very sensitive with the time instant t. It is also clear from Figs. 12 and 13 that the behavior of the thermal stresses is the most affected by the change of time. The temperature also increases with the increase in time to a certain range and then gradually decreases again with the passage of time.

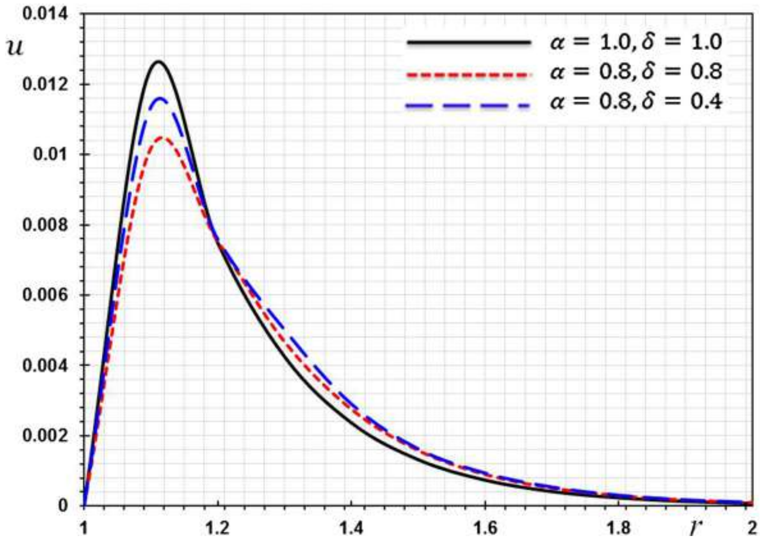

Fig. 7 The variation of displacement u with different values of the fractional parameters δ, α

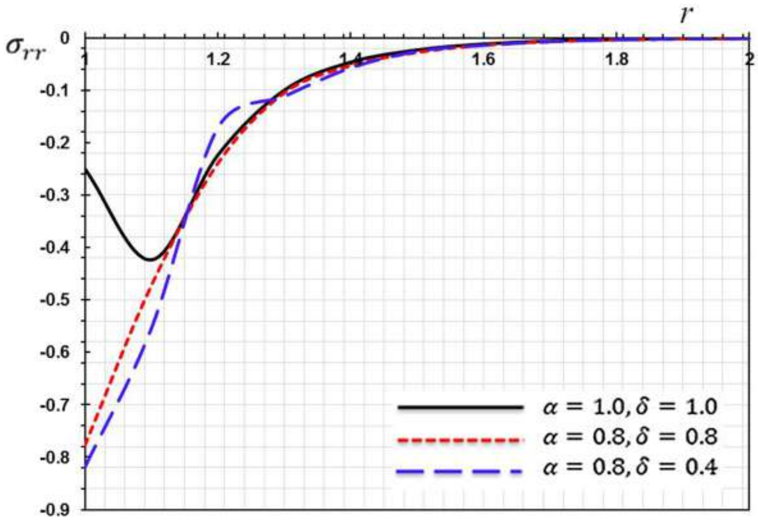

Fig. 8 The variation of the stress σ_{rr} with different values of the fractional parameters δ, α

8 Conclusion

In the context of this paper, generalized thermoviscoelastic fractional model (FMVDPL) with multi-phase-lag and parameter α is investigated. This model has widely used in chemistry, biology, modeling and identification, electronics, wave propagation, and viscoelasticity [10–15]. In the limited cases, the proposed model reduces to various classical, generalized, fractional thermoelasticity models (see Sect. 6). According to this model, the distributions of the physical quantities for an isotropic homogeneous spherical cavity of radius a whose

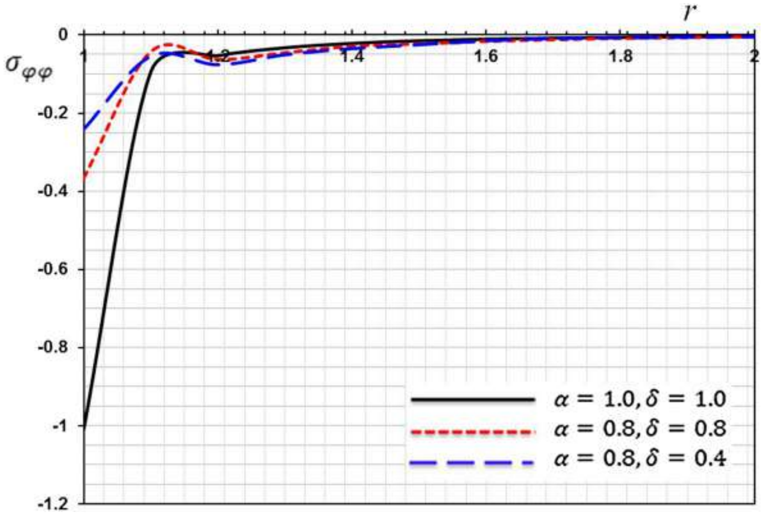

Fig. 9 The variation of the stress $\sigma_{\varphi\varphi}$ with different values of the fractional parameters δ,α

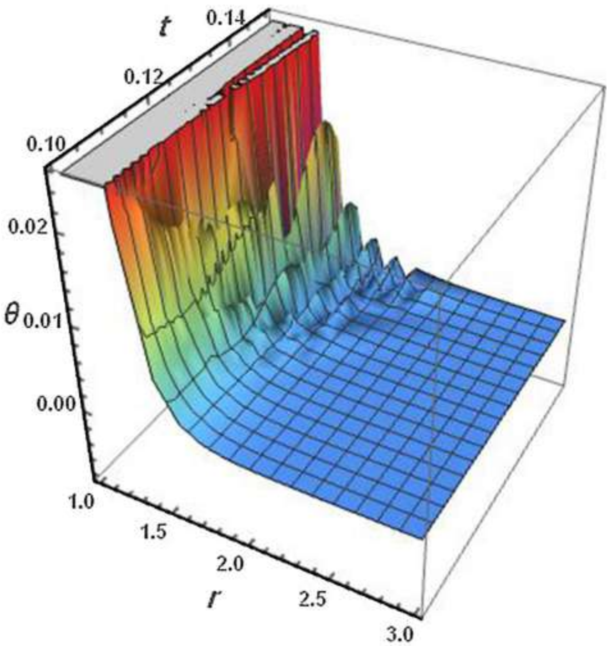

Fig. 10 The temperature θ with different times

inner surface is subjected to a time-dependent varying heat and constrained are discussed. Numerical simulation results yield the following conclusions:

- The effects of the fractional parameter α, δ on all the physical fields under consideration are very obvious.

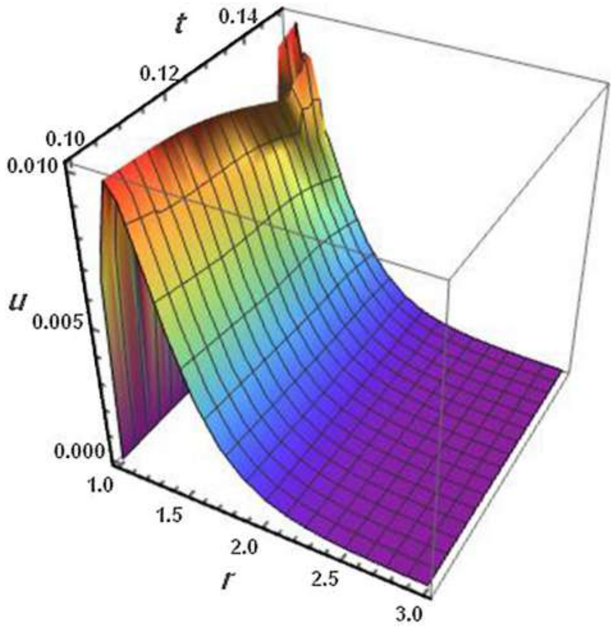

Fig. 11 The displacement u with different times

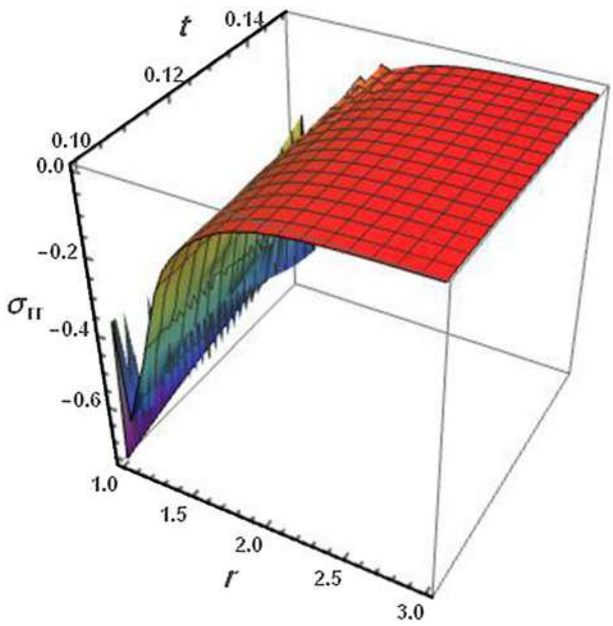

Fig. 12 The radial stress σ_{rr} with different times

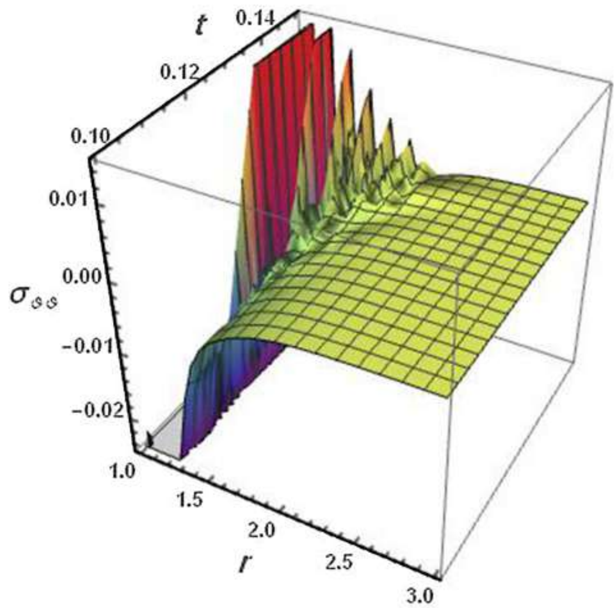

Fig. 13 The hoop stress $\sigma_{\vartheta\vartheta}$ with different times

- The results of our study differ from the generalized theory with dual-phase-lags (DPL) of the phenomenon of limited velocities of the propagation of heat waves and the Kelvin–Voigt model of thermoviscoelasticity.
- The obtained results are very useful for the material science researchers and material designers who are working on the development of the thermoviscoelasticity and fractional thermoviscoelasticity models.
- The technique introduced in this study is important in real-life engineering problems and mathematical biology models according to the fractional time derivative.

Data Availability Statement This manuscript has associated data in a data repository. [Authors' comment: All data generated or analysed during this study are included in this published article [and its supplementary information files].]

Authors' contributions All the authors have made substantive contributions to the article and assume full responsibility for its content. The authors read and approved the final manuscript.

Funding Not applicable.

Compliance with ethical standards

Conflict of interest The authors declare that they have no conflict of interest.

References

1. M. Biot, J. Appl. Phys. **27**, 240 (1956)
2. H. Lord, Y. Shulman, J. Mech. Phys. Solids **15**, 299 (1967)
3. A.E. Green, K.A. Lindsay, J. Elasticity **2**, 1 (1972)
4. A.E. Green, P.M. Naghdi, Proc. Roy. Soc. Lond. A **432**, 171 (1991)
5. A.E. Green, P.M. Naghdi, J. Elasticity **31**, 189 (1993)
6. D.Y. Tzou, Annual Rev. Heat Transf. **4**, 111 (1992)
7. D.Y. Tzou, J. Heat Transf. **117**, 8 (1995)
8. D.Y. Tzou, Int. J. Heat Mass Transf. **38**, 3231 (1995)
9. D.S. Chandrasekharaiah, Appl. Mech. Rev. **51**, 705 (1998)
10. R.L. Bagley, P.J. Torvik, J. Rheol. **27**, 201 (1983)
11. R.C. Koeller, Trans. ASME-J. Appl. Mech. **51**, 299 (1984)
12. R. Huilgol, N. Phan-Thien, (Elsevier Amsterdam, 1997)
13. A. A. Ilioushin, B. E. Pobedria, (Nauka Moscow, 970)
14. K.K. Kalkal, S. Deswal, J. Mech. **30**, 383 (2014)
15. M. Kanoria, S.H. Mallik, Eur. J. Mech. A/Solid. **29**, 695 (2010)
16. Y.A. Rossikhin, Appl. Mech. Rev. **50**, 15 (1997)
17. I. Podlubny, Academic Press, (New York, 1999)
18. K. S. Miller, B. Ross, (Wiley, New York, 1993)
19. Y.Z. Povstenko, Mech. Res. Commun. **37**, 436 (2010)
20. H.H. Sherief, A.M.A. El-Sayed, A.M. Abd El-Latief, Int. J. Solids Struct. **47**, 269 (2010)
21. M.A. Ezzat, Phys. B **405**, 4188 (2010)
22. M.A. Ezzat, Phys. B **406**, 30 (2011)
23. G. Jumarie, Comput. Math Appl. **59**, 1142 (2010)
24. A.S. El-Karamany, M.A. Ezzat, J. Therm. Stress. **34**, 264 (2011)
25. A.E. Abouelregal, Waves Random Complex Media (2019). https://doi.org/10.1080/17455030.2019.1628320
26. A.E. Abouelregal, J. Appl. Comput. Mech. (2019). https://doi.org/10.22055/jacm.2019.29960.164
27. A.E. Abouelregal, Mater. Res. Exp. (2019). https://doi.org/10.1088/2053-1591/ab447f
28. A.E. Abouelregal, M.A. Elhagary, A. Soleiman, K.M. Khalil, Mech. Based Des. Struct. Mach. (2020). https://doi.org/10.1080/15397734.2020.1730189
29. J.C. Mishra, S.C. Samanta, A.K. Chakrabarty, Int. J. Eng. Sci. **29**, 1209 (1991). https://doi.org/10.1016/0020-7225(91)90025-x
30. D.S. Mashat, A.M. Zenkour, A.E. Abouelregal, Int. J. Acoust. Vib. **22**, 260 (2017)
31. G. Honig, U. Hirdes, J. Comput. Appl. Math. **10**, 13 (1984)
32. M.I.A. Othman, A.E. Abouelregal, Microsyst. Technol. **23**, 5635 (2017)